Berezinskii-Kosterlitz-Thouless Phase of a Driven-Dissipative Condensate

NA YOUNG KIM WOLFGANG H. NITSCHE YOSHIHISA YAMAMOTO

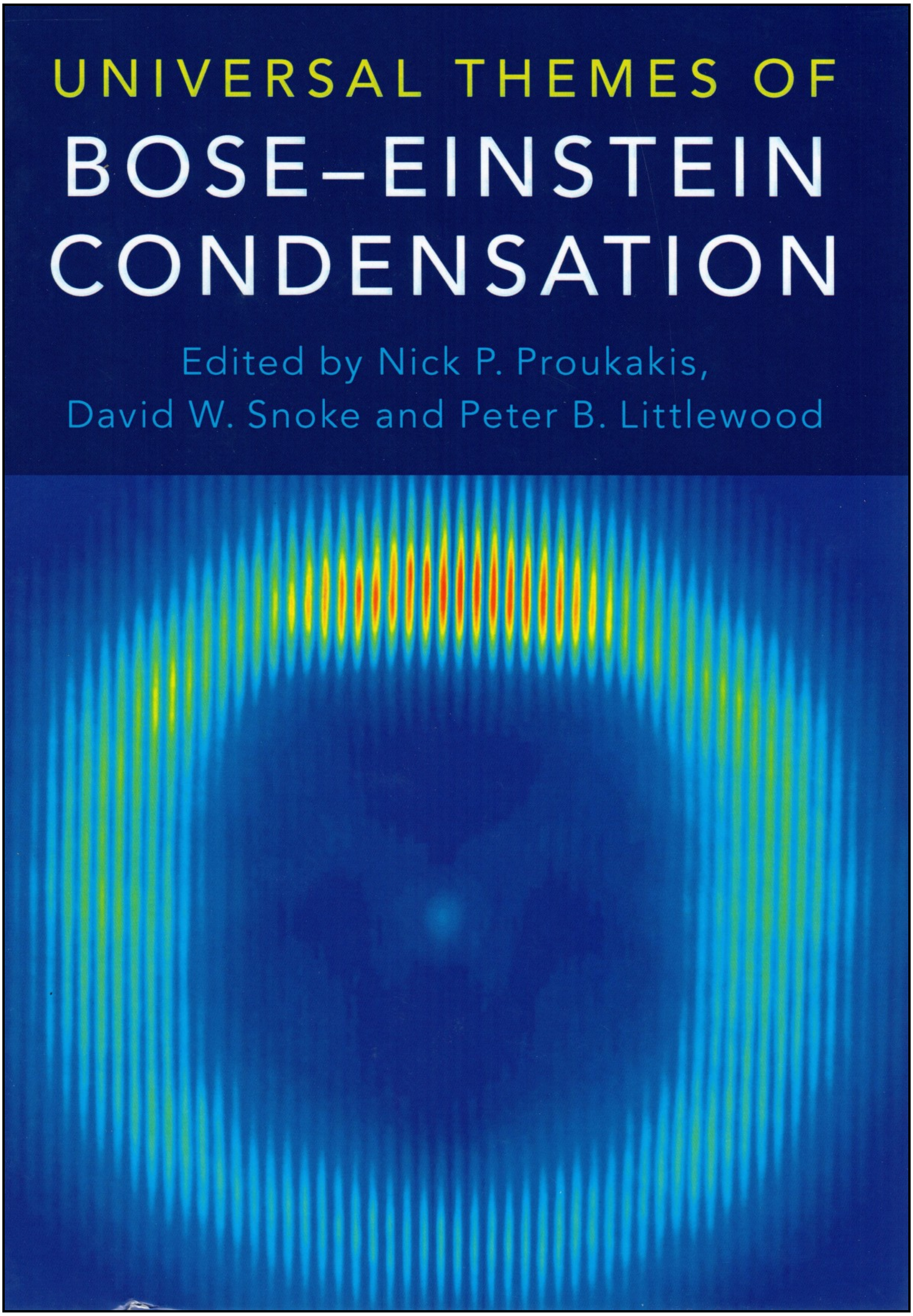

UNIVERSAL THEMES OF BOSE-EINSTEIN CONDENSATION

NICK P. PROUKAKIS
Newcastle University

DAVID W. SNOKE
University of Pittsburgh

PETER B. LITTLEWOOD
University of Chicago

CAMBRIDGE UNIVERSITY PRESS

CAMBRIDGE
UNIVERSITY PRESS

University Printing House, Cambridge CB2 8BS, United Kingdom

One Liberty Plaza, 20th Floor, New York, NY 10006, USA

477 Williamstown Road, Port Melbourne, VIC 3207, Australia

4843/24, 2nd Floor, Ansari Road, Daryaganj, Delhi – 110002, India

79 Anson Road, #06–04/06, Singapore 079906

Cambridge University Press is part of the University of Cambridge.

It furthers the University's mission by disseminating knowledge in the pursuit of education, learning, and research at the highest international levels of excellence.

www.cambridge.org
Information on this title: www.cambridge.org/9781107085695
10.1017/9781316084366

First published 2017

Printed in the United Kingdom by TJ International Ltd. Padstow Cornwall

A catalogue record for this publication is available from the British Library

Library of Congress Cataloging-in-Publication Data
Names: Proukakis, Nick, editor. | Snoke, David W., editor. | Littlewood, Peter B., editor.
Title: Universal themes of Bose-Einstein condensation / edited by Nick P. Proukakis (Newcastle University), David W. Snoke (University of Pittsburgh), Peter B. Littlewood (University of Chicago).
Description: Cambridge, United Kingdom ; New York, NY : Cambridge University Press, 2017. | Includes bibliographical references and index.
Identifiers: LCCN 2016039245| ISBN 9781107085695 (Hardback ; alk. paper) | ISBN 1107085691 (Hardback ; alk. paper)
Subjects: LCSH: Bose-Einstein condensation.
Classification: LCC QC175.47.B65 U55 2017 | DDC 530.4/2–dc23
LC record available at https://lccn.loc.gov/2016039245

ISBN 978-1-107-08569-5 Hardback

10

Berezinskii-Kosterlitz-Thouless Phase of a Driven-Dissipative Condensate

NA YOUNG KIM
Edward L. Ginzton Laboratory, Stanford University, California, USA
Present address: Institute for Quantum Computing, Department of Electrical and Computer Engineering, University of Waterloo, Canada

WOLFGANG H. NITSCHE
Edward L. Ginzton Laboratory, Stanford University, California, USA
Present address: Halliburton, Houston, Texas, USA

YOSHIHISA YAMAMOTO
Edward L. Ginzton Laboratory, Stanford University, California, USA
Japan Science and Technology Agency, Chiyoda-ku, Tokyo, Japan

Microcavity exciton-polaritons are interacting Bose particles which are confined in a two-dimensional (2D) system suitable for studying coherence properties in an inherently nonequilibrium condition. A primary question of interest here is whether a true long-range order exists among the 2D exciton-polaritons in a driven open system. We give an overview of theoretical and experimental works concerning this question, and we summarize the current understanding of coherence properties in the context of Berezinskii-Kosterlitz-Thouless transition.

10.1 Introduction

Strange but striking phenomena, which are accessed by advanced experimental techniques, become a fuel to stimulate both experimental and theoretical research. Experimentalists concoct new tools for sophisticated measurements, and theorists establish models in order to explain the surprising observation, ultimately expanding our knowledge boundary. A classic example of the seed to the knowledge expansion is the feature of abnormally high heat conductivity in liquid helium reported by Kapitza and Allen's group, who used cryogenic liquefaction techniques in 1938 [1, 2]. It is a precursor to a "resistance-less flow" a new phase of matter, coined as superfluidity in the He-II phase. Immediately after this discovery, London conceived a brilliant insight between superfluidity and Bose-Einstein condensation (BEC) of noninteracting ideal Bose gases [3], which has led to establish the concept of coherence as off-diagonal long-range order emerging in the exotic states of matter. Since then, it is one of the core themes in equilibrium Bose systems to elucidate the intimate link of superfluidity and BEC in natural and artificial materials, where dimensionality and interaction play a crucial role in determining the system phase.

Let us consider the noninteracting ideal Bose gases whose particle number N is fixed in a three-dimensional box with a volume V. According to the Bose-Einstein statistics, the average occupation number N_i in the state i with energy ϵ_i is given by $N_i = 1/(e^{\beta(\epsilon_i-\mu)} - 1)$ with the chemical potential μ and a temperature parameter $1/\beta = k_B T$ (Boltzmann constant k_B and temperature T). For the positive real number of N_i, μ is restricted to be smaller than ϵ_i, and the ground-state particle number N_0 diverges as μ approaches the lowest energy ϵ_0. Its thermodynamic phase transition refers to BEC, in which the macroscopic occupation in the ground state is represented by the classical field operator $\Psi(\mathbf{r}, t) = \sqrt{n(\mathbf{r}, t)}e^{i\phi(\mathbf{r},t)}$, where $n(\mathbf{r}, t)$ is the particle density and $\phi(\mathbf{r}, t)$ is the phase. The critical temperature T_c is defined as a temperature at which particles are accumulated in the ground state, while the number of particles in excited states would be finite [4, 5]. The definite phase in the BEC manifests spontaneous spatial coherence by virtue of spontaneous symmetry breaking in the system. The spatial coherence is quantified by the first-order coherence function $g^{(1)}(\mathbf{r}_1, t_1, \mathbf{r}_2, t_2)$ at different spatial $(\mathbf{r}_1, \mathbf{r}_2)$ and time (t_1, t_2) coordinates. By definition, we express the $g^{(1)}(\mathbf{r}_1, t_1, \mathbf{r}_2, t_2)$ function in the normalized form in terms of $\Psi(\mathbf{r}, t)$:

$$g^{(1)}(\mathbf{r}_1, t_1, \mathbf{r}_2, t_2) = \frac{\left\langle \Psi^\dagger(\mathbf{r}_1, t_1)\, \Psi(\mathbf{r}_2, t_2)\right\rangle}{\sqrt{\left\langle \Psi^\dagger(\mathbf{r}_1, t_1)\, \Psi(\mathbf{r}_1, t_1)\right\rangle \left\langle \Psi^\dagger(\mathbf{r}_2, t_2)\, \Psi(\mathbf{r}_2, t_2)\right\rangle}}. \qquad (10.1)$$

In equilibrium, the time dependence is suppressed in Eq. (10.1), and we apply the particle distribution in momentum space $n(\mathbf{k})$ via Fourier transform using $\Psi(\mathbf{k}) = (2\pi\hbar)^{-\frac{3}{2}} \int d\mathbf{r}\Psi(\mathbf{r}) \exp(i\mathbf{k} \cdot \mathbf{r}))$. Then, the numerator of Eq. (10.1) is reduced to a simple formula, $\left\langle \Psi^\dagger(\mathbf{r}_1)\, \Psi(\mathbf{r}_2)\right\rangle = V^{-1} \int d\mathbf{k}\, \langle n(\mathbf{k})\rangle \exp(-i\mathbf{k} \cdot (\mathbf{r}_1 - \mathbf{r}_2))$. Below the critical temperature, the momentum distribution $n(\mathbf{k}) = N_0\delta(\mathbf{k}) + \sum_{\mathbf{k}\neq 0} n(\mathbf{k})$ has the dominant ground-state term, which reduces the integral in the numerator to be N_0. Consequently, the $g^{(1)}$-function converges to a constant value of N_0/N even at a large distance limit, $r = |\mathbf{r}_1 - \mathbf{r}_2| \to \infty$. This attribute is known to be off-diagonal long-range order (ODLRO) arising from the constant condensate fraction.

In real systems, we should consider various sources of fluctuations, which populate particles at excited states apart from the condensates. Furthermore, the particle interaction and the system dimension are crucial to determine ODLRO. Theoretically, Hohenberg, Mermin, and Wagner reached a conclusion that the true long-range order is impossible in low-dimensional noninteracting Bose gases at finite temperatures, which is known as the Hohenberg-Mermin-Wagner theorem [6, 7].

Namely, the spatial coherence in the large distance limit is zero in infinite 1D and 2D systems, where thermal fluctuations completely destroy the ODLRO. However, Berezinskii, Kosterlitz, and Thouless in the early 1970s conjectured a topological phase order which exhibits coherence and superfluidity in 2D systems [8, 9]. The Berezinskii-Kosterlitz-Thouless (BKT) theory is considered to be central for identifying the relation of superfluidity in diverse materials systems. This chapter is organized as follows: in Section 10.2, we review the fundamental physics of the BKT phase and introduce major material systems to unveil the BKT phase. Sections 10.3 and 10.4 discuss both theoretical and experimental activities on the BKT phase in microcavity exciton-polaritons under the nonequilibrium condition. We finish by examining the current status of the BKT research efforts followed by prospective remarks on proposed experimental schemes in order to reach the conclusive results. A closely related theoretical discussion of the nature of the phase transition in 2D polariton condensates is given in Chapter 11 by Keeling et al.

10.2 Berezinskii-Kosterlitz-Thouless Physics

At zero temperature, the perfect phase coherence exists in the free bosons as the true ODLRO associated with BEC; however, at finite temperature, we pay attention to several factors for identifying coherence properties: the system dimensionality, the system size, and particle interaction. Given the focus of the chapter, we limit our discussion to 2D, whose energy density of states is constant even at the zero energy. Hence, in principle, BEC is impossible in a 2D uniform system with continuous symmetry due to a large number of particles occupied in all the excited states. On the other hand, the density of states in spatially confined systems can vanish for a specific potential profile; consequently, BEC can be restored in a finite-sized 2D system.

When we take the repulsive interaction among particles into account in 2D Bose fluids, the story becomes profound. Berezinskii, Kosterlitz, and Thouless studied the 2D XY model for low-temperature ordered states in the infinite system, which may apply to spin crystals and superfluid helium, superconducting materials, and 2D atoms [8, 9]. The so-called quasicoherence in the BKT phase forms in the infinite system for weakly interacting Bose fluids and the coherence nature of weakly interacting Bose fluids in the finite-sized system are currently studied for trapped atoms and microcavity exciton-polaritons. Recently, Hadzibabic's group managed to control the interaction strengths in a gas trapped in a harmonic potential. They confirmed the observation of the BKT phase in this 2D finite system consisting of interacting Bose atoms [10]. Table 10.1 summarizes the system order with respect to the system size and the particle interactions at nonzero temperature in 2D.

Table 10.1 *Summary of 2D phases in terms of system size and interaction at finite temperatures.*

$T \neq 0$	2D finite system	2D infinite system
zero interaction	ODLRO/BEC	no ODLRO/no BEC
weak repulsive interaction	BKT	BKT

10.2.1 Quasi-Long-Range Order

Thermal fluctuations indeed disturb a well-defined phase of coherent particles, and the degree of phase fluctuations becomes appreciable if the density fluctuations are suppressed by the particle–particle interaction. Two major mechanisms to control the spatial coherence are thermally excited phonons and topological defects, "vortices" [11, 12]. Vortices have zero particle density at their core and quantized angular momentum with a continuous phase rotation of $2\pi n$ around the core. Singly charged vortices with $n = 1$ (for a vortex) and $n = -1$ (for an antivortex) are primarily relevant in coherent condensates since multicharged vortices with $|n| > 1$ will rapidly dissociate into several single-charged vortices. Two forms of vortices exist in the condensates: free vortices or bound vortex–antivortex pairs. Their influence over the system phase is dissimilar: whereas the circulating phase of free vortices kills the spatial coherence of the system where free vortices flow around, the bound pairs of vortex–antivortex have no effect on the phase as a result of the mutual cancellation between oppositely rotating phases. Hence, such pairs do not alter the coherence over large distances.

From a thermodynamic point of view, a vortex–antivortex pair is energetically favorable over a free vortex. Both a single free vortex and a vortex–antivortex pair increase the entropy S by an amount approximately proportional to the logarithm of the system size. However, while a free vortex also increases the energy E by an amount proportional to the logarithm of the system size, a vortex–antivortex pair gives a finite energy contribution which is independent of the system size. With respect to the free energy $F = E - TS$ in a large 2D condensate, the presence of vortex–antivortex pairs is always advantageous, and free vortices exist only above a critical temperature, T_{BKT} [11]. The low-temperature state of a condensate, where all vortices are paired up, is called the BKT phase [8, 9]. The only remaining mechanism to contribute to a decay of the spatial coherence in the BKT phase is the thermal excitation of phononic phase fluctuations, which leads to the decay of the spatial coherence with a slow power law of the form:

$$g^{(1)}(\mathbf{r}_1, t, \mathbf{r}_2, t) \propto |\mathbf{r}_1 - \mathbf{r}_2|^{-a_{\mathrm{p}}}, \qquad (10.2)$$

where the exponent $a_p = (n_s \lambda_T^2)^{-1}$ depends only on the superfluid density n_s and the thermal wavelength $\lambda_T = h/\sqrt{2\pi m_{\text{eff}} k_B T}$ [11].

We can derive the upper limit of a_p in equilibrium by assuming a vortex with a core radius ξ in the center of a superfluid with radius R and effective particle mass m_{eff}. The energy E of a free vortex is calculated by integrating the local kinetic energy of the superfluid flow as

$$E = \int \frac{m_{\text{eff}} n_s(\mathbf{r})}{2} (v(\mathbf{r}))^2 d^2\mathbf{r} = n_s \lambda_T \frac{k_B T}{2} \ln\left(\frac{R}{\xi}\right), \quad (10.3)$$

and the entropy S of a vortex is proportional to the logarithm of the number of positions as

$$S = k_B \ln\left(\frac{\pi R^2}{\pi \xi^2}\right) = 2k_B \ln\left(\frac{R}{\xi}\right). \quad (10.4)$$

The overall free energy F of the vortex has a simple expression,

$$F = E - TS = (n_s \lambda_T^2 - 4) \frac{k_B T}{2} \ln\left(\frac{R}{\xi}\right). \quad (10.5)$$

If $n_s \lambda_T^2 < 4$, F is negative since the rest terms are all positive, thus the BKT threshold is determined by $n_s \lambda_T^2 = 4$, which separates two phases drawn in Fig. 10.1. The excitation of the first free vortices reduces n_s [13], making the creation of more free vortices even easier, and eventually superfluidity disappears [11]. The BKT state with the bound vortex–antivortex pairs possesses superfluidity, and a flowing condensate experiences friction through the excitation

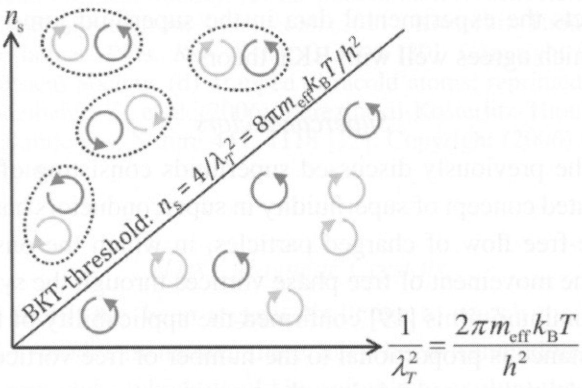

Figure 10.1 Diagram of equilibrium BKT transition. At high superfluid density n_s and low-temperature T, spatial coherence appears over long distances where only vortex–antivortex pairs exist. Decreasing n_s or increasing T causes the system to cross the BKT threshold where the vortices unbind, which destroys the spatial coherence.

Table 10.2 *Decay mechanisms of the coherence in 2D superfluids.*

$0 < T < T_{BKT}$		$T > T_{BKT}$
phonons slow decay of coherence	vortex–antivortex pairs no decay of coherence	free vortices fast decay of coherence
quasi-long-range order		no ODLRO

of quasiparticles (i.e., phonons) whose dispersion relation is a form of $\epsilon_{\text{excitation}} \approx v\,|\mathbf{p}_{\text{excitation}}|$. The Landau criterion [14, 15, 16, 17] tells us that such excitations can only be created if the condensate flows with a velocity above v. Decay mechanisms of the coherence in 2D superfluids are summarized in Table 10.2.

Four representative physical systems are under the active investigation to search the BKT phase both in experiments and theories, and Fig. 10.2 collects the captured features of the BKT phases in their measurable parameters: liquid He, superconductors, photons, and cold atoms.

Liquid Helium

The first direct observation of the BKT state succeeded in liquid helium films by Bishop and Reppy [18, 21]. In these experiments, thin ^{4}He films have been absorbed on a substrate with a high-quality torsional oscillator. If the system is cooled below the transition temperature, the oscillation period of the mechanical system increases since the superfluid He decouples from the rest of the mechanical system. From the period shift, superfluid density and dissipation are determined unambiguously. Fig. 10.2a collects the experimental data in the superfluid jump along transition temperatures, which agrees well with BKT theory.

Superconductors

Different from the previously discussed superfluids consisting of electric neutral particles, the related concept of superfluidity in superconductors has been described as the resistance-free flow of charged particles, in which the onset of resistance corresponds to the movement of free phase vortices through the system [22]. Measurements on aluminum films [19] confirmed the applicability of the BKT theory, and the DC resistance is proportional to the number of free vortices shown in Fig. 10.2b. Superconductivity occurs below the transition temperature, and it has also been suggested [23] that at low temperatures, the vortices and antivortices in a superconductor form a 2D crystal structure, similar to ions in a standard crystal. In this case, the system becomes resistive once the vortex–antivortex crystal starts to melt.

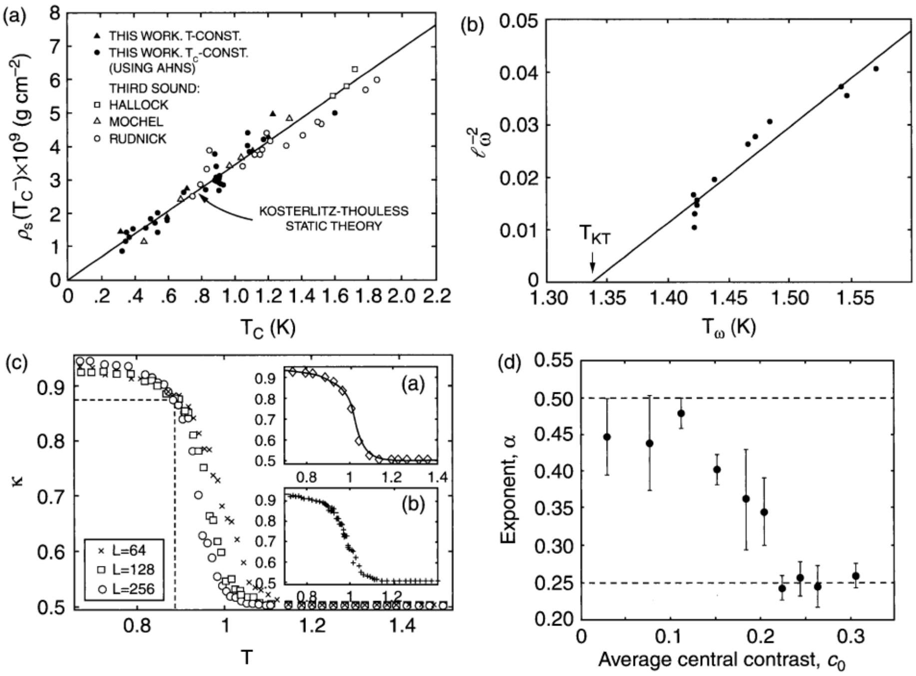

Figure 10.2 Experimental signatures of the BKT crossover captured in different physical systems: (a) He-II phase; reprinted with permission from Bishop, D. J., and Reppy, J. D. (1978), Study of the superfluid transition in two-dimensional ^{4}He films, *Phys. Rev. Lett.*, **40**, 1727 [18]. Copyright (1978) by the American Physical Society. (b) Superconductors; reprinted with permission from Hebard, A. F., and Fiory, A. T. (1980), Evidence for the Kosterlitz-Thouless transition in thin superconducting aluminum films, *Phys. Rev. Lett.*, **44**, 291 [19]. Copyright (1980) by the American Physical Society. (c) 2D photon lattices with Kerr nonlinearity; reprinted with permission from Small, et al. (2011), Kosterlitz-Thouless crossover in a photonic lattice. *Phys. Rev. A*, **83**, 013806 [20]. Copyright (2011) by the American Physical Society. (d) Trapped ultracold atoms; reprinted with permission from Hadzibabic, Z., et al. (2006), Berezinskii-Kosterlitz-Thouless crossover in a trapped atomic gas, Nature **441**, 1118 [12]. Copyright (2006) by the Nature Publishing Group.

2D XY Magnetic Crystals

Despite the fact that it has been a great challenge to search the ideal material to study the 2D XY model in nature, there have been tremendous efforts to grow layered magnetic crystals, which would be suitable to explore the BKT phase transition in 2D [24]. The same 2D BKT physics applies to these materials such as $BaNi_2(PO_4)_2$; namely, a long-range order induced by the vortex–antivortex pair would exhibit signatures of diverging magnetic susceptibility and a broad peak in the magnetic specific heat. Recently, there is a report by Putsch et al. that similar signatures in magnetic properties are observed in a Cu-based spin-dimer crystal, $C_{36}H_{48}Cu_2F_6N_8O_{12}S_2$ induced by a magnetic field [25].

Photonic Systems

The BKT crossover has been also addressed in a 2D nonlinear photonic medium. Since the nonlinear Schrödinger equation to describe the nonlinear photonics system is mathematically equivalent to the 2D spin XY model, we can engineer 2D photonic lattices to create the optical analog BKT phase transition and to observe the associated unbinding of vortices. Such lattices can be realized as a nonlinear 2D waveguide array, where the effective temperature is controlled by the initial randomness. Simulations confirmed the proliferation of free vortices above the transition temperature [20]. Experimental work was reported in a nonlinear optical system comprising light traveling through a nonlinear crystal, with the observation of the creation of free vortices above a critical temperature [26].

Atomic Bose Gases

Interference measurements between 2D gases of ultracold atoms demonstrated quasicoherence at low temperatures. The temperature rise induces a loss of the coherence, which is accompanied by the appearance of vortices identified in the interference patterns, confirming the predictions of the BKT theory [12]. These measurements used a strongly interacting Bose gas. Weakly interacting Bose gases start with the normal state and first go through a transition into an intermediate state which exhibits quasi-long-range order without superfluidity before finally undergoing a second transition into the BKT state with superfluidity and a quasi-long-range order [27].

The superfluidity of a 2D atomic BKT condensate has clearly been demonstrated by stirring such a condensate with a laser beam which behaves like a solid obstacle due to repulsive interaction [28, 29]. Finally, the bound vortex–antivortex pairs in an atomic 2D BKT gas have been observed by measuring the shadow which the condensate casts when illuminated with light at the resonance frequency of the atoms [30]. The exponent values of the power-law decay are plotted against the average interference contrast, reaching $1/4$, the theoretical value in equilibrium BKT physics (Fig. 10.2d). Related concepts of scale invariance in 2D atomic gases are discussed in Chapter 9 by Chin.

10.2.2 BKT Physics in Exciton-Polariton Systems

Besides the aforementioned platforms, microcavity exciton-polaritons (reviewed in Chapter 4 by Littlewood and Edelman) are primary quasiparticles in the strongly coupled photon and quantum-well (QW) exciton systems, which are regarded as quantum fluids. In low-density limit, they are composite bosons governed by Bose-Einstein statistics. Since the discovery in the monolithically grown semiconductor microcavity-QW structure [31], condensation and its coherence character have been studied using inorganic and organic semiconductors for the last two decades [32, 33]. Inherited from underlying entities, photons and excitons, the resulting exciton-polaritons are short-lived due to the extremely short photon lifetime, and they are scattered by repulsive Coulomb exchange interaction among fermions. Their effective mass is on the order of 10^{-4} electron mass, and they can dwell on the order of 1–100 ps inside the cavity. Hence, it is inevitable to refill exciton-polaritons, which naturally leak through the cavity as the open-dissipative system. This very nature of the 2D confinement in a planar QW-microcavity and the open-dissipativeness adds a rich context to explore the BKT physics in microcavity exciton-polaritons. Both theorists and experimentalists have been actively scrutinizing the search of steady-state coherent states and superfluidity.

10.3 Theoretical Studies of Exciton-Polaritons

Appreciating the nonequilibrium character of exciton-polaritons, theorists have addressed a series of fundamental questions: the existence of steady-state spontaneous condensation by repeated pump-decay processes, distinct signatures of nonequilibrium condensation compared with the equilibrium case, and the effect of fluctuations, which lead to the computation of spatial correlations in the context of BKT physics. Szymanska et al. set a Hamiltonian to describe a system, a bath and the system-bath interaction including pump and decay terms. The self-consistent solution for steady-state spontaneous condensation emerges even in the nonequilibrium condition. The excitation spectra induced by the diffusive phase mode are calculated as shown in Fig. 10.3a; the different correlations, decay would be expected from the diffusive phase mode [38]. The authors presented the extensive follow-up work in the mean-field theory to construct the phase map [34] (see also Chapter 4).

Discussed in the introduction, the spatial coherence is enumerated by the first-order correlation function. The principal mechanisms to affect the coherence property yield the different asymptotic behavior of the first-order correlation function in the long-distance limit. Thus, the long-distance decay will be a clue to identifying the prevailing mechanism. Tsyplyatyev and Whittaker computed the shape of the first-order coherence function in 1D depending on the known mechanisms [39]. Following the standard procedure, the authors found that $g^{(1)}(x)$ has a Gaussian form for nonzero momentum distributions in a trap, whereas

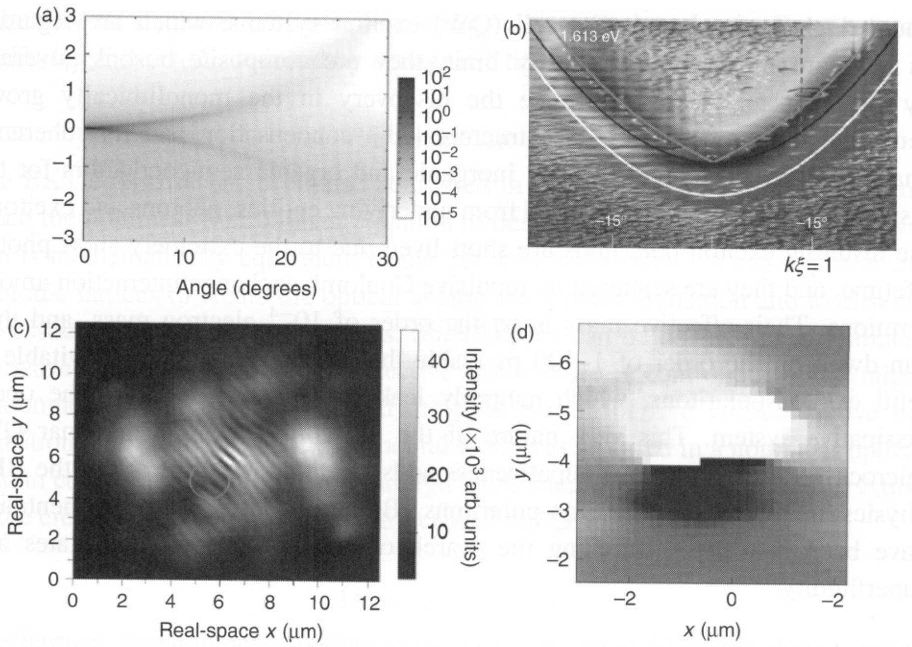

Figure 10.3 (a) Theoretically computed excitation spectra of exciton-polaritons. Reprinted with permission from Szymańska, M. H., et al. (2007), Mean-field theory and fluctuation spectrum of a pumped decaying Bose-Fermi system across the quantum condensation transition, *Phys. Rev. B*, **75**, 195331 [34]. Copyright (2007) by the American Physical Society. (b) Experimentally measured Bogoliubov linear spectra from a trapped polariton. Reprinted with permission from Utsunomiya, S., et al. (2008), Observation of Bogoliubov excitations in exciton-polariton condensates, *Nat. Phys.*, **4**, 700 [35]. Copyright (2008) by the Nature Publishing Group. (c) Interferograms of a pinned vortex in a CdTe-polariton system. Reprinted with permission from Lagoudakis, K. G., et al. (2008), Quantized vortices in an exciton-polariton condensate, *Nat. Phys.*, **4**, 706 [36]. Copyright (2008) by the Nature Publishing Group. (d) The extracted phase map of the vortex–antivortex pair in a GaAs-microcavity sample. Reprinted with permission from Roumpos, G., et al. (2011), Single vortex-antivortex pair in an exciton-polariton condensate, *Nat. Phys.*, **7**, 129 [37]. Copyright (2011) by the Nature Publishing Group.

$g^{(1)}(x)$ decays exponentially both for localization and polariton-interaction with the coherence length.

There are also several recent theoretical papers which target 2D superfluidity with the emphasis of nonequilibrium nature in exciton-polariton condensates [40, 41, 42]. Altman et al. inquired if effective equilibrium ODLRO emerges in driven 2D isotropic Bose systems or not. By mapping a nonequilibrium condensate system to an effective equilibrium system, the authors concluded that algebraic order appears at an intermediate length scale and the true ODLRO completely disappears by nonlinearity to cause nonequilibrium fluctuations [40] (see also discussion in Chapter 11). On the other hand, Chiocchetta and Carusotto developed a phenomenological model in terms of the linearized stochastic Gross-Pitaevskii equation to compute a spatial correlation function given density and phase fluctuations. They claimed that in 2D, the power-law form of the correlation function appears at the long-distance limit as a BKT phase transition [41]. In the optical parametric oscillator regime, Dagvadorj and colleagues were able to simulate the BKT phase transition to trace vortex–antivortex pairs and the unbound vortices across the pump thresholds [42]. They also calculated first-order spatial correlations, whose long-range behavior shows the exponential decay below threshold but the algebraic decay above threshold. The power-law exponent values are pump-power dependent and approximately 1.4, which is much higher than 0.25, the maximum value in the equilibrium counterpart near the threshold, to 0 at a higher threshold, indicating the true ODLRO in the exciton-polariton systems.

10.4 Experimental Work with Exciton-Polaritons

Exciton-polaritons are captured from reflectivity measurements on a semiconductor QW-microcavity based on GaAs, where the anticrossing of energy states appears at the coupled exciton-photon regions [31]. Soon after the first report in 1992, there have been numerous theoretical works to predict the quantum Bose nature and experimental ones to observe its experimental signatures for last two decades. We encourage readers to refer to Chapter 1 for a brief overview of the early history and associated challenges by Snoke et al. Exciton-polaritons naturally decay through the leakage of photons out of the cavity, and these photons preserve the microscopic information of decaying exciton-polaritons in terms of energy, in-plane momentum, and polarization. Due to the extremely light effective mass of $10^{-4} \sim 10^{-5}$ times the elementary electron mass, the condensation temperatures of GaAs and CdTe semiconductors lie around 4 $\sim$10 K, and they can be at room temperatures for GaN and inorganic semiconductors. Exciton-polaritons indeed exhibit common features similar to equilibrium quantum fluids in addition to exclusive signatures of the nonequilibrium setting.

10.4.1 Superfluidity

Quantum mechanical effects become pronounced when the primary length scale of particle is on the order of thermal de Broglie wavelength given by λ_T. At a low density, exciton-polaritons undergo a phase transition to Bose condensates with spontaneous phase symmetry breaking. Experimental signatures are accumulated to understand dynamical nature of condensation due to a finite lifetime: nonlinear threshold behavior in the occupation of the zero momentum state and spectral narrowing above threshold, and spontaneous coherence [46, 43, 47]. Subsequently, the search for superfluidity in exciton-polaritons began. Fig. 10.3b displays the Bogoliubov-like phonon excitation spectra reported in trapped exciton-polaritons by an incoherent pumping [35]. In a coherent excitation pumping to set a parametric oscillator regime, the flow velocity of exciton-polariton fluids is measured against the defect [15], which would be well explained by the famous Landau criterion. Hydrodynamic solitons propagate at the defects in exciton-polariton superfluids [16]. Quantized vortices (Fig. 10.3c) [36], half-quantum vortices [48], and a bound vortex–antivortex pair (Fig. 10.3d) [37] are clearly seen in coherent exciton-polariton condensates through interferometric measurement. Unfortunately, time-integrated interferometric measurements are a limitation to capturing spontaneous formation of free vortices and bound vortex–antivortex pairs, which would be the direct evidence of the BKT phase transition.

10.4.2 Spatial Coherence

Across the BKT phase transition, in addition to the spontaneous formation of bound vortex–antivortex pairs, another manifestation occurs in the long-distance asymptotic behavior of the first-order spatial correlation function introduced in Section 10.1. In order to construct the phase map and to measure the spatial coherence of the condensate, two standard types of interferometers were commonly used to measure spatial coherence: the Michelson interferometer (Fig. 10.4a) [43, 44] and Young's double-slit interferometer (Fig 10.4b) [50, 45]. The visibility of the interferograms is directly mapping to the $g^{(1)}(x, -x)$ functions presented in Fig. 10.4c, d. Although both methods provide spatial dependence, the Michelson one is convenient to yield the 2D map with improved spatial resolution fixed by a detector pixel size. Hence, the spatial dependence in the $g^{(1)}(x, -x)$ function is extensively measured using the Michelson interferometer in general whose simple schematic is drawn in Fig. 10.4a.

The dense $g^{(1)}(x, -x)$-function 2D maps with GaAs QW-embedded microcavity samples are reported in Refs. [44, 49]. Note that the two works deploy different pumping profiles: a top-hat pump spot and a Gaussian pump spot. In both excitation schemes, at the first-order phase transition, the sharp emergence of superfluid density occurs at a specific pump power to excite exciton-polaritons, and a power-law decay of the spatial coherence is observed in both measurements. However, the exponent values of the power law from the fitting are very different: the power-law exponent is above 1 for the top-hat profile, which exceeds the maximum

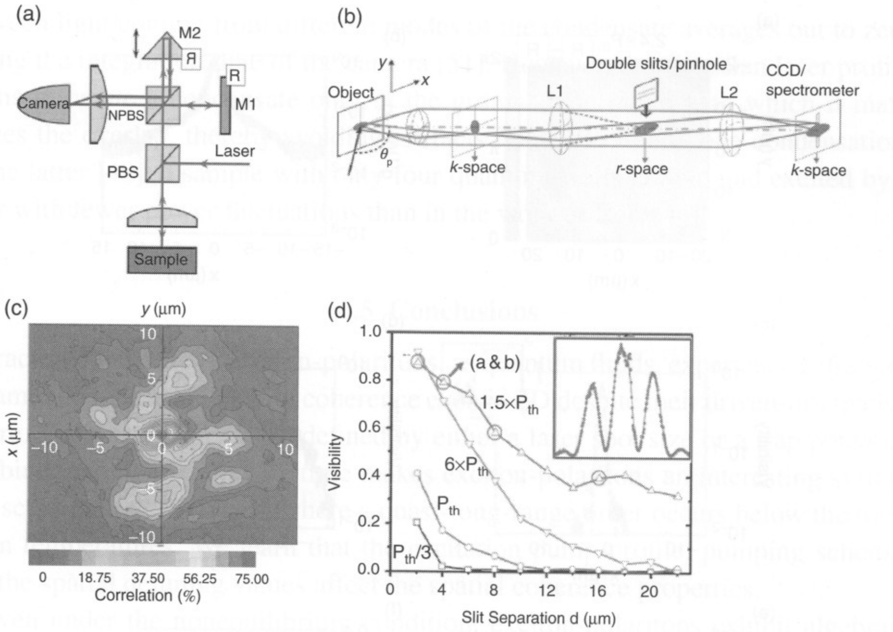

Figure 10.4 Schematics of (a) a Michelson interferometer and (b) Young's double-slit interferometer. (c) Spontaneous spatial coherence of the CdTe condensates taken by the Michelson interferometer in Ref. [43]. (d) The visibility of Young's interference peaks from the GaAs condensates at different pump-power values. (a) reprinted with permission from Roumpos, G., et al. (2012), Power-law decay of the spatial correlation function in exciton-polariton condensates, *Proc. Natl. Acad. Sci.*, **109**, 6467 [44]. Copyright (2012) National Academy of Sciences, USA. (b) and (d) reprinted with permission from Lai, C. W., et al. (2007), Coherent zero-state and π-state in an exciton-polariton condensate array, *Nature*, **450**, 529 [45]. Copyright (2007) by the Nature Publishing Group. (c) reprinted with permission from Kasprzak, J., et al. (2006), Bose-Einstein condensation of exciton polaritons. *Nature*, **443**, 409. [43]. Copyright (2006) by the Nature Publishing Group.

value, $1/4$ for a BKT condensate in thermal equilibrium [44]. On the other hand, the observed exponent of the power-law signals using the Gaussian pump profile is $\approx 1/4$ near the condensation threshold and becomes $<1/4$ at higher particle densities [49].

In addition, the exponent in the earlier work [44] by Roumpos et al. seemed to increase slightly at higher exciton-polariton densities, whereas the theory predicts it to decrease. This article argued that the unexpected large exponent might be a result of having a nonequilibrium condensate due to the continuous creation and decay of exciton-polaritons. Later, Nitsche and the team found that a top-hat excitation profile invariably results in simultaneous condensation in multiple modes, which leads to a faster decay of the measured spatial coherence since any interference

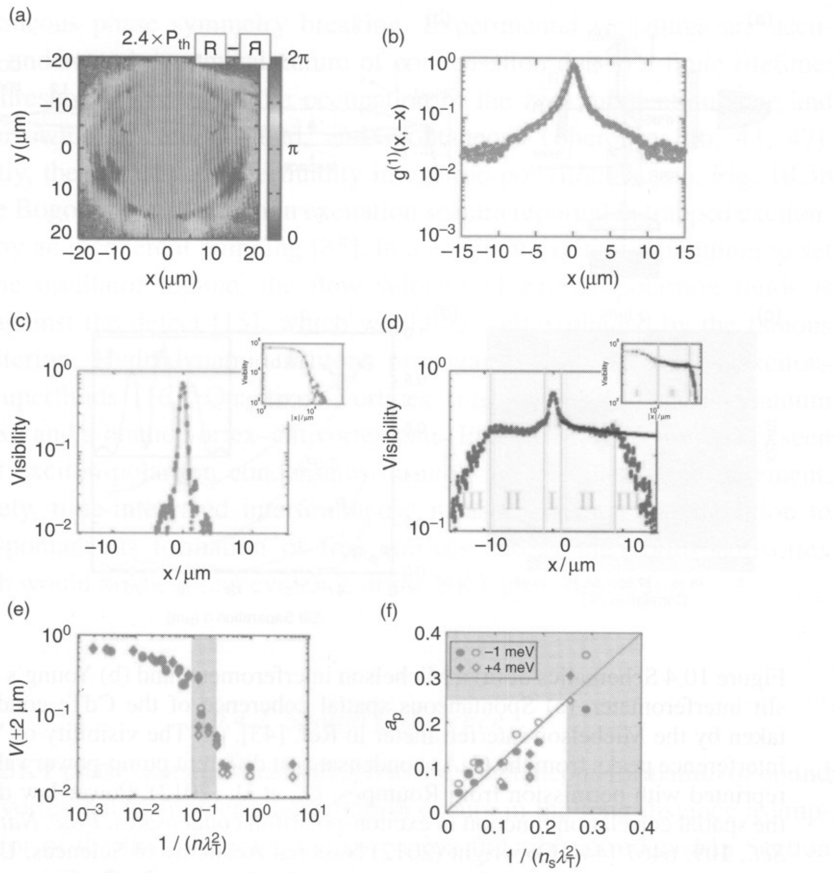

Figure 10.5 (a) A representative visibility above threshold from the interference between the reference image and the retro-reflective image. Reprinted with permission from Roumpos, G., et al. (2012), Power-law decay of the spatial correlation function in exciton-polariton condensates, *Proc. Natl. Acad. Sci.*, **109**, 6467 [44]. Copyright (2012) National Academy of Sciences, USA. (b) A semi-log scale plot of the first-order spatial correlation function under the top-hat pump profile with the Gaussian and power-law fit (dotted line) in Ref. [44]. Using the Gaussian pump profile, the interference visibility shows different shapes in space (c) below and (d) above threshold. The lines in (c) and (d) are the Gaussian fit, and the line in (d) is the power-law fit. (e) Visibility and (f) the power-law exponent a_p are plotted in terms of the total density n and the superfluid density n_s. Panels (b)–(f) are reprinted with permission from Nitsche, W. H., et al. (2014), Algebraic order and the Berezinskii-Kosterlitz-Thouless transition in an exciton-polariton gas, Phys. Rev. B **90**, 205430 [49]. Copyright (2014) by the American Physical Society.

between light coming from different modes of the condensate averages out to zero during the integration time of the camera [51]. However, the Gaussian laser profile seems to create a condensate only in the ground-state mode with which it maximizes the overlap, thereby avoiding artifacts related to multimode condensation. In the latter [49], a sample with only four quantum wells is used and excited by a laser with fewer power fluctuations than in the work of Ref. [44].

10.5 Conclusions

Interacting microcavity exciton-polaritons, as quantum fluids, experience a thermodynamic phase transition with coherence even in 2D despite their driven-dissipative nature. The finite system size defined by either a laser spot size or a trap potential combined with their short lifetime makes exciton-polaritons an interesting system to discuss the BKT physics, where a quasi-long-range order occurs below the transition temperatures. We learn that the excitation pump profile, pumping scheme, and the spatial detuning values affect the spatial coherence properties.

Even under the nonequilibrium condition, exciton-polaritons exhibit algebraic order with the power-decay form. Recently, theoretical models in a particular pumping scheme [40, 41] offer support for the experimental findings regarding the power-law decay of correlation functions; yet a microscopic theory needs to be developed in order to apply for nonresonant excitation cases, which still remains as a calculation-heavy challenge. Experimentally, we have had no luck with observing the spontaneous formation of vortices and bound vortex pairs across phase transition for the unequivocal claim of the BKT transition. This is the next target in decoding the clear relation between the true long-range-ordered state and the quasi-long-range order in dynamical exciton-polariton condensates.

References

[1] Allen, J. F., and Misener, A. D. 1938. Flow of liquid helium II. *Nature*, **141**, 75.

[2] Kapitza, P. 1938. Viscosity of liquid helium below the λ-point. *Nature*, **141**, 74.

[3] London, F. 1938. The λ-phenomenon of liquid helium and the Bose-Einstein degeneracy. *Nature*, **141**, 643–644.

[4] Anderson, M. H., Ensher, J. R., Matthews, M. R., Wieman, C. E., and Cornell, E. A. 1995. Observation of Bose-Einstein condensation in a dilute atomic vapor. *Science*, **269**, 198–201.

[5] Davis, K. B., Mewes, M.-O., Andrews, M. R., van Druten, N. J., Durfee, D. S., Kurn, D. M., and Ketterle, W. 1995. Bose-Einstein condensation in a gas of sodium atoms. *Phys. Rev. Lett.*, **75**, 3969–3973.

[6] Mermin, N. D., and Wagner, H. 1966. Absence of ferromagnetism or antiferromagnetism in one- or two-dimensional isotropic Heisenberg models. *Phys. Rev. Lett.*, **17**, 1133–1136.

[7] Hohenberg, P. C. 1967. Existence of long-range order in one and two dimensions. *Phys. Rev.,* **158**, 383–386.

[8] Berezinskii, V. L. 1972. Destruction of long-range order in one-dimensional and two-dimensional systems possessing a continuous symmetry group. II. Quantum systems. *Soviet Journal of Experimental and Theoretical Physics*, **34**, 610–616.

[9] Kosterlitz, J. M., and Thouless, D. J. 1973. Ordering, metastability and phase transitions in two-dimensional systems. *Journal of Physics C Solid State Physics*, **6**, 1181–1203.

[10] Fletcher, R. J., Robert-de Saint-Vincent, M., Man, J., Navon, N., Smith, R. P., Viebahn, K. G. H., and Hadzibabic, Z. 2015. Connecting Berezinskii-Kosterlitz-Thouless and BEC phase transitions by tuning interactions in a trapped gas. *Phys. Rev. Lett.*, **114**, 255302.

[11] Hadzibabic, Z., and Dalibard, J. 2011. Two-dimensional Bose fluids: an atomic physics perspective. *Riviesta del Nuovo Cimento*, **34**, 389–433.

[12] Hadzibabic, Z., Krüger, P., Cheneau, M., Battelier, B., and Dalibard, J. 2006. Berezinskii-Kosterlitz-Thouless crossover in a trapped atomic gas. *Nature*, **441**, 1118–1121.

[13] Leggett, A. J. 1999. Superfluidity. *Rev. Mod. Phys.*, **71**, S318–S323.

[14] Landau, L. D., and Lifshitz, E. M. 1959. *Fluid Mechanics*. Pergamon Press.

[15] Amo, A., Lefrère, J., Pigeon, S., Adrados, C., Ciuti, C., Carusotto, I., Houdré, R., Giacobino, E., and Bramati, A. 2009. Superfluidity of polaritons in semiconductor microcavities. *Nature Physics*, **5**, 805–810.

[16] Amo, A., Pigeon, S., Sanvitto, D., Sala, V. G., Hivet, R., Carusotto, I., Pisanello, F., Leménager, G., Houdré, R., Giacobino, E., Ciuti, C., and Bramati, A. 2011. Polariton superfluids reveal quantum hydrodynamic solitons. *Science*, **332**, 1167–1170.

[17] Kavokin, A., Baumberg, J. J., Malpuech, G., and Laussy, F. P. 2011. *Microcavities*. Oxford Science Publications. Oxford University Press.

[18] Bishop, D. J., and Reppy, J. D. 1978. Study of the superfluid transition in two-dimensional ^{4}He films. *Phys. Rev. Lett.*, **40**, 1727–1730.

[19] Hebard, A. F., and Fiory, A. T. 1980. Evidence for the Kosterlitz-Thouless transition in thin superconducting aluminum films. *Phys. Rev. Lett.*, **44**, 291–294.

[20] Small, Eran, Pugatch, Rami, and Silberberg, Yaron. 2011. Berezinskii-Kosterlitz-Thouless crossover in a photonic lattice. *Phys. Rev. A*, **83**, 013806.

[21] Bishop, D. J., and Reppy, J. D. 1980. Study of the superfluid transition in two-dimensional ^{4}He films. *Phys. Rev.*, **22**, 5171–5185.

[22] Beasley, M. R., Mooij, J. E., and Orlando, T. P. 1979. Possibility of vortex-antivortex pair dissociation in two-dimensional superconductors. *Phys. Rev. Lett.*, **42**, 1165–1168.

[23] Gabay, Marc, and Kapitulnik, Aharon. 1993. Vortex–antivortex crystallization in thin superconducting and superfluid films. *Phys. Rev. Lett.*, **71**, 2138–2141.

[24] Regnault, L. P., and Rossat-Mignod, J. 1990. *Magnetic Properties of Layered Transition Metal Compounds*. Physics and Chemistry of Materials with Low-Dimensional Structures, vol. 9. Kluwer Academic Publishers. Chap. Phase transitions in quasi-two-dimensional planar magnets, pages 271–321.

[25] Tutsch, U., Wolf, B., Wessle, S., Postulka, L., Tsui, Y., Jeschke, H.O., Opahle, I., Saha-Dasgupta, T., Valenti, R., Bruhl, A., Removic-Langer, K., Kretz, T., Lerner, H.-W., Wagner, M., and Lang, M. 2014. Evidence of a field-induced Berezinskii-Kosterlitz-Thouless scenario in a two-dimensional spin-dimer system. *Nature Comm.*, **5**, 5169.

[26] Situ, G., Muenzel, S., and Fleischer, J. W. 2013. Berezinskii-Kosterlitz-Thouless transition in a photonic lattice. *arXiv:1304.6980*, Apr.

[27] Cladé, P., Ryu, C., Ramanathan, A., Helmerson, K., and Phillips, W. D. 2009. Observation of a 2D Bose gas: from thermal to quasicondensate to superfluid. *Phys. Rev. Lett.*, **102**, 170401.

[28] Campbell, G. K. 2012. Quantum gases: superfluidity goes 2D. *Nature Physics*, **8**, 643–644.

[29] Desbuquois, R., Chomaz, L., Yefsah, T., Léonard, J., Beugnon, J., Weitenberg, C., and Dalibard, J. 2012. Superfluid behaviour of a two-dimensional Bose gas. *Nature Physics*, **8**, 645–648.

[30] Choi, J.-y., Seo, S. W., and Shin, Y.-i. 2013. Observation of thermally activated vortex pairs in a quasi-2D Bose gas. *Phys. Rev. Lett.*, **110**, 175302.

[31] Weisbuch, C., Nishioka, M., Ishikawa, A., and Arakawa, Y. 1992. Observation of the coupled exciton–photon mode splitting in a semiconductor quantum microcavity. *Phys. Rev. Lett.*, **69**, 3314–3317.

[32] Deng, H., Haug, H., and Yamamoto, Y. 2010. Exciton-polariton Bose-Einstein condensation. *Rev. Mod. Phys.*, **82**, 1489–1537.

[33] Byrnes, T. Kim, N. Y., and Yamamoto, Y. 2014. Exciton-polariton condensates. *Nature Physics*, **10**, 803–813.

[34] Szymańska, M. H., Keeling, J., and Littlewood, P. B. 2007. Mean-field theory and fluctuation spectrum of a pumped decaying Bose-Fermi system across the quantum condensation transition. *Phys. Rev. B*, **75**, 195331.

[35] Utsunomiya, S., Tian, L., Roumpos, G., Lai, C. W., Kumada, N., Fujisawa, T., Kuwata-Gonokami, M., Löffler, A., Höfling, S., Forchel, A., and Yamamoto, Y. 2008. Observation of Bogoliubov excitations in exciton-polariton condensates. *Nature Physics*, **4**, 700–705.

[36] Lagoudakis, K. G., Wouters, M., Richard, M., Baas, A., Carusotto, I., André, R., Dang, L. S., and Deveaud-Plédran, B. 2008. Quantized vortices in an exciton-polariton condensate. *Nature Physics*, **4**, 706.

[37] Roumpos, G., Fraser, M. D., Löffler, A., Höfling, S., Forchel, A., and Yamamoto, Y. 2011. Single vortex–antivortex pair in an exciton-polariton condensate. *Nature Physics*, **7**, 129–133.

[38] Szymańska, M. H., Keeling, J., and Littlewood, P. B. 2006. Nonequilibrium quantum condensation in an incoherently pumped dissipative system. *Phys. Rev. Lett.*, **96**, 230602.

[39] Tsyplyatyev, O., and Whittaker, D. M. 2012. Spatial coherence of a polariton condensate in 1D acoustic lattice. *Physica Status Solidi B Basic Research*, **249**, 1692–1697.

[40] Altman, Ehud, Sieberer, Lukas M., Chen, Leiming, Diehl, Sebastian, and Toner, John. 2015. Two-dimensional superfluidity of exciton polaritons requires strong anisotropy. *Phys. Rev. X*, **5**, 011017.

[41] Chiocchetta, A., and Carusotto, I. 2013. Non-equilibrium quasi-condensates in reduced dimensions. *Europhysics Letters*, **102**, 67007.

[42] Dagvadorj, G., Fellows, J. M., Matyjaśkiewicz, S., Marchetti, F. M., Carusotto, I., and Szymańska, M. H. 2015. Nonequilibrium phase transition in a two-dimensional driven open quantum system. *Phys. Rev. X*, **5**, 041028.

[43] Kasprzak, J., Richard, M., Kundermann, S., Baas, A., Jeambrun, P., Keeling, J. M. J., Marchetti, F. M., Szymańska, M. H., André, R., Staehli, J. L., Savona, V., Littlewood, P. B., Deveaud, B., and Dang, L. S. 2006. Bose-Einstein condensation of exciton polaritons. *Nature*, **443**, 409–414.

[44] Roumpos, G., Lohse, M., Nitsche, W. H., Keeling, J., Szymańska, M. H., Littlewood, P. B., Löffler, A., Höfling, S., Worschech, L., Forchel, A., and Yamamoto, Y. 2012. Power-law decay of the spatial correlation function in exciton-polariton condensates. *Proceedings of the National Academy of Science*, **109**, 6467–6472.

[45] Lai, C. W., Kim, N. Y., Utsunomiya, S., Roumpos, G., Deng, H., Fraser, M. D., Byrnes, T., Recher, P., Kumada, N., Fujisawa, T., and Yamamoto, Y. 2007. Coherent zero-state and π-state in an exciton-polariton condensate array. *Nature*, **450**, 529–532.

[46] Deng, H., Weihs, G., Santori, C., Bloch, J., and Yamamoto, Y. 2002. Condensation of semiconductor microcavity exciton polaritons. *Science*, **298**, 199–202.

[47] Balili, R., Hartwell, V., Snoke, D., Pfeiffer, L., and West, K. 2007. Bose-Einstein condensation of microcavity polaritons in a trap. *Science*, **316**, 1007–1010.

[48] Lagoudakis, K. G., Ostatnický, T., Kavokin, A. V., Rubo, Y. G., André, R., and Deveaud-Plédran, B. 2009. Observation of half-quantum vortices in an exciton-polariton condensate. *Science*, **326**, 974–976.

[49] Nitsche, Wolfgang H., Kim, Na Young, Roumpos, Georgios, Schneider, Christian, Kamp, Martin, Höfling, Sven, Forchel, Alfred, and Yamamoto, Yoshihisa. 2014. Algebraic order and the Berezinskii-Kosterlitz-Thouless transition in an exciton-polariton gas. *Phys. Rev. B*, **90**, 205430.

[50] Deng, H., Solomon, G. S., Hey, R., Ploog, K. H., and Yamamoto, Y. 2007. Spatial coherence of a polariton condensate. *Phys. Rev. Lett.*, **99**, 126403.

[51] Nitsche, Wolfgang H., Kim, Na Young, Roumpos, Georgios, Schneider, Christian, Höfling, Sven, Forchel, Alfred, and Yamamoto, Yoshihisa. 2016. Spatial correlation of two-dimensional bosonic multimode condensates. *Phys. Rev. A*, **93**, 053622.